Design and prototyping of a fluid-antenna system

Malika Gabdullina, B. Eng. in Electrical and Computer Engineering

Submitted in fulfilment of the requirements
for the degree of Master of Science in
Electrical and Computer Engineering

Department of Electrical and Computer Engineering
School of Engineering and Digital Science
Nazarbayev University

53 Kabanbay Batyr Avenue,
Astana, Kazakhstan, 010000

Lead Supervisor: Dr. Sultangali Arzykulov
Co-supervisor: Dr. Refik Kizilirmak

April 2025

Abstract

In this master thesis, we aim to develop a hardware prototype for a reconfigurable fluid antenna system (FAS) operating at 2.4 GHz. By applying different liquid-metal-controlling methods, the optimal output characteristics of FAS will be obtained and analyzed. Different actuation techniques will be implemented and analyzed to identify the optimal configurations for key antenna parameters. The process for designing fluid-antenna will be also presented. The performance of the fabricated prototype will be thoroughly characterized and analyzed to validate its reconfigurability and assess its potential for enhanced wireless communication. The proposed prototype strategy can be used in hardware implementations of other technologies and find many applications.

Table of content

List of Figures

List of Tables

Chapter 1 – Introduction

1.1 Introduction

Fifth-generation wireless communication technologies have been broadly implemented recently. Despite this, the industry is already striving to develop and implement more advanced next-generation technology with better performance. After all, in modern cities, the growing number of smart devices and data-intensive applications has led to a growing demand for spectrum efficiency [1]. Traditional antennas are impractical to support this demand due to their limited size. Therefore, metamaterials have long been studied to create next-generation antennas [2].

Fluid-antenna system (FAS) is the one of the most promising technologies for the upcoming generation. It is a fast and simple liquid-structure that can adjust the performance parameters of the antenna via software control. The use of a fluid in antenna design provides the possibillity to overcome the basic design constraints of the solid antennas and raise the bar for wireless network performance. Such technologies can also be used to improve the efficiency of other technologies [3]. Moreover, it is believed that FASs will also contribute to overcome the massive connectivity challenge of previous generation antennas [4].

Research of FAS is beginning to become a significant technology and already has great potential. However, there are still lack of prototypes of the antenna and their hardware implementation cases. That is why, it is important to offer physical model of the fluid-antenna in addition to theoretical knowledge.

This research will provide a comprehensive review of state-of-the-art fluid-antenna designs. In addition, we will build our hardware design based on a theoretical FAS model developed in [5]. One of the possible designs according to this model is presented in Figure 1.1.

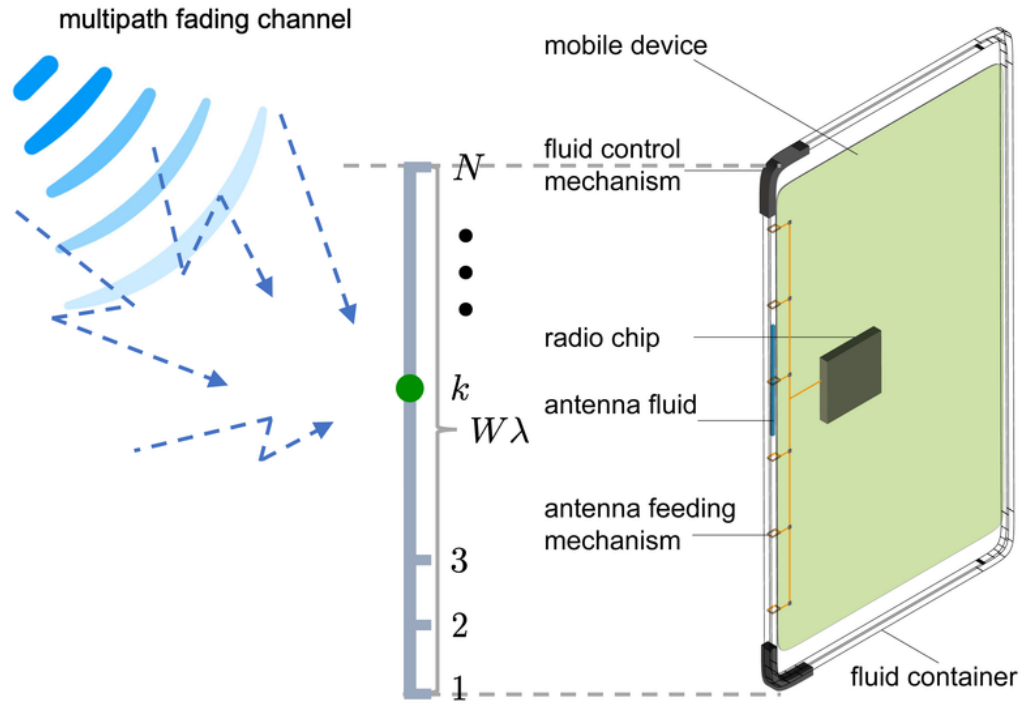

Figure 1.1: A possible architecture of FAS according to theoretical model.

1.2 Literature review

The increasing demand for versatile and adaptable wireless communication systems has driven the development of reconfigurable antennas. Among the emerging technologies, fluid antennas have garnered significant attention due to their potential for dynamic tuning and novel material applications [6]. Therefore, the development of fluid-antenna technologies is of great importance for the field. Unlike existing traditional antennas, they provide a completely new performance due to their liquid nature. While traditional antennas are designed to operate on a fixed frequency band, with consistent radiation pattern and polarization, the use of liquid materials as an antenna will allow it to reconfigure their performance parameters [6].

The realization of fluid antennas critically depends on the selection and utilization of appropriate materials, particularly the fluid component itself [7]. Therefore, a comprehensive understanding of the material properties and their impact on antenna performance is important.

Although there are two types of liquid antennas: metallic and non-metallic [9], this section would be the primary focus on the metallic liquids.

1.2.1 Liquid metals

Most research of fluid-antenna focuses on liquid metals, which are also called “conductive” liquids [9], [10]. Liquid conductive metals because of their solid-like oxide skin on the surface, provide mechanical stability to the antennas and hence, provide flexibility while maintaining high conductivity suitable for antenna applications.

The first metallic liquid to be employed in antenna design was mercury [11]. The construction of reconfigurable metallic liquid antennas is made possible by Mercury's fluidic and conductive properties. However, due to the toxicity and flammability of mercury [12], finding another material was important for a breakthrough in the development of liquid antennas. This breakthrough was Gallium-based alloys like Galinstan or eutectic gallium indium (EGaIn). Such alloys combine excellent parameters such as low melting point, non-toxicity and high electrical conductivity, which is crucial for a liquid antenna [13].

Graphene is the most recent material to be reported for antenna design; its electrical, thermal, and optical properties make it a viable choice in a number of applications. Nevertheless, graphene metallic liquid has not been used in the existing research for antenna design [14].

The selection of an appropriate conductive fluid is a first step in developing fluid antenna designs. Table 1 presents a comprehensive analysis of fluids considered conductive enough for use as radiative elements in antennas. Their diverse material properties provide the initial parameters to consider in creating fluid antenna design.

Table 1. Comprehensive review of liquid metals for the fluid-antenna material

Liquid metal	Conductive (S/m)	Composition	Melting point (^oC)	Density (g/cm^3)
Mercury	1.0×10^6	Pure Hg	-39	13.55
EGaIn	3.4×10^6	75% Ga, 25% In	16	6.28
Galinstan	3.3×10^6	68.5% Ga, 21.5% In, 10% Sn	-19	6.44
GaIn10Ink	3.0×10^6	~90% Ga, ~10% In, 0.026% O	16	6.36
Graphene	50×10^6	Graphene	Does Not melt	2.26

The next section is a discussion of the various reconfigurable antenna technologies that enable dynamic control over antenna parameters, including mechanical, electrical, and material-based approaches. These technologies are crucial for translating the inherent potential of fluid materials into practical and adaptable antenna systems.

1.2.2 Reconfigurable FAS

Reconfigurable antenna technologies cover a variety of methods for achieving dynamic control over antenna characteristics. Researchers show that the implementation of fluid-antenna systems opens up the opportunities for reconfigurability by changing the physical size of the antenna. For example, it allows the antenna to be used for flexible or wearable electronics without the fear of being broken [15]. Also, it allows for a less complex antenna design due to the fact that a separate electrical circuit block is not required for tunability such as radio frequency switches, micro-electromechanical system switches or three-layer semiconductor diodes [16]. The use of

liquids enables the antennas to be easily implemented for frequency, gain, radiation pattern, polarization or compound reconfigurability.

The ability to reconfigure antenna parameters is achieved by controlling the conductive fluid flow in cavities. The conventional method is to actuate the liquid mechanically to change the physical parameters of the fluid antenna. Generally, such techniques use the pressure to move conductive fluid. One of them is a liquid pump, which is widely used in the design of fluid-antennas in [16]. It demonstrated that because liquid metal antennas have a more flexible antenna structure variation, their tuning range in terms of frequency and radiation pattern is significantly broader than that of conventional antennas. On the other hand, the fabrication process of liquid metal antennas is typically more complex than that of conventional ones, and the pump-based tunable system's temporal response is significantly slower than that of the electrical tuning system. Another controlling method can be achieved by using electrical actuations [17]. The advantage over the mechanical methods is that electrical actuators are easier to integrate with other systems. This technique is based on manipulating with the surface or interfacial tension of the conductive fluid by applying the voltage difference and consists of following methods [18]: 1) electrocapillary actuation (ECA); 2) continuous electrowetting; 3) electrochemically controlled capillary (ECC); and 4) electrowetting on dielectric. Additionally, embedding fluid switches within the antenna structure is another attractive method.

Reconfigurability of the liquid antenna can be achieved in a wide range of antenna parameters. This section focuses primarily on the frequency-tuning, and liquid-switch aspects of the antennas.

1.2.3 Frequency-reconfigurable antennas

The resonant frequency is usually reconfigured by altering the effective electrical length of the radiating patch. This can be achieved by changing its physical length [19] or by introducing slots that elongate the resonant current path [20]. By using fluid conductive to alter the length of the antenna, it is possible to tune the resonant frequency.

Monopole antennas are frequently reported such [18], [19], [21], because their resonant frequency is directly proportional to their length, and this can be easily changed using LM. In [22] frequency-reconfigurability of monopole antenna was controlled by using unidirectional micropumps, and achieved tunable operation in the range of 1.29 to 5.17 GHz. However, this design utilized mercury as the liquid metal despite this toxic nature and failed to operate while using Ga-alloys, which limits its application.

Another monopole antenna that is frequency-tunable through its stretching capability was studied in [23]. This antenna also showed frequency tuning from 0.88 GHz to 0.72 GHz in the length range of 7 mm to 10 mm without any significant losses. The setup of this antenna is presented in Figure 1.2. The antenna fabricated by using silicon-based Ecoflex polymer with Galinstan liquid metal as well. The Ecoflex is very soft material, which is crucial for developing a stretchable antenna. In [24], a liquid metal position in the fluidic channel of a monopole stub antenna was controlled by a syringe, connected to the end of the tube to inject or withdraw it by applied air. To easily control the liquid metal, it was necessary to add HCl-treatment to the Galinstan before using. As a result, liquid metal flexibly changes between two positions, providing reversible frequency tuning. Despite the successful experiment, the actuation part of the design isn't automatic, which made it less applied.

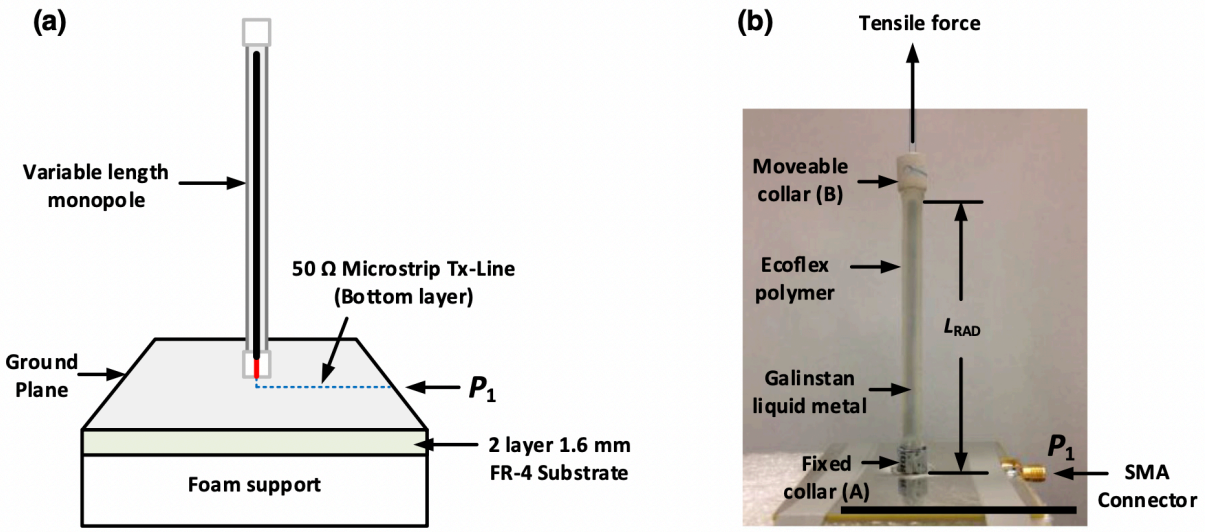

Figure 1.2: Experimental setup of stretchable frequency-reconfigurable antenna: a) schematic; b) actual setup.

1.2.4 Fluid Switches

In [25], a pattern-reconfigurable patch antenna using liquid metal is presented. The specific of this design, that there is a switchable ground technique. It is based on the adding or removing of the liquid metal in the different segments of the ground plane. Notably, not only is the ground plane switchable, but there are five switchable beams that could be filled by the liquid metal or emptied and reconfigure the performance of the antenna. As a result, it is capable of switching its beams with very low scan loss. In the letter, the liquid position was altered by using a syringe, but different actuation techniques were proposed to be developed further.

A lot of the previous work reviewed in this article focuses on concept demonstrations rather than the practicality and implementation of the actuation. There is still a long way to go to develop and optimize the actuation techniques for circuits and antennas.

1.3 Research objectives

Initial aim of this research is to develop a design of a fluid-antenna system operating at 2.4 GHz, including antenna design by Computer Simulation Technology Studio Suite (CST Studio Suite), antenna controller unit design and fabrication of hardware prototype of the system. The research will mostly focus on understanding how to design the fluid-antenna with adaptive tunable structure. The design characteristics of the system will be comprehensively reviewed. This will provide the optimal antenna design parameters.

Next aim of this research is to fabricate the prototype of the antenna and experimentally evaluate it. Additionally, this aim validates the theoretical concept proposed on [5].

1.4 Methodology

This section outlines the methodologies used in the research and consists of three main parts: selection of the design parameters, computational simulation of the antenna and controller unit and its fabrication.

1.4.1 Antenna design parameters

To accurately select the antenna design parameters, it is necessary to a analyze the existing literature, to understand the weak area of the current researches. Moreover, it is crucial to analyze all the advantages and challenges from reviewed studies and determine the optimal. After all, monopole antenna design approach was developed. The design parameters were obtained by using theoretical calculations.

1.4.2 Computational simulations and optimization techniques

Next step of the antenna development is computational simulations of antenna design, developed in previous step. CST Studio Suite software was used for that aim. The simulations

were conducted to evaluate the following antenna characteristics: S_{11}-parameter over frequency, antenna gain, radiation pattern.

In this step antenna design parameters were also optimized by using parametric sweep technic. Using this technic, the influence of parameters such element spacing, monopole length and diameter on antenna performance was obtained.

When it comes to designing the controller unit, the Tinkercad Circuits modelling program was used. In the initial design of the controller unit, the liquid-metal drop's movement was controlled by the Arduino Uno microcontroller with the H-bridge circuit. This scheme presented in Figure 1.3 allow to control the voltage and polarity applied across the channel.

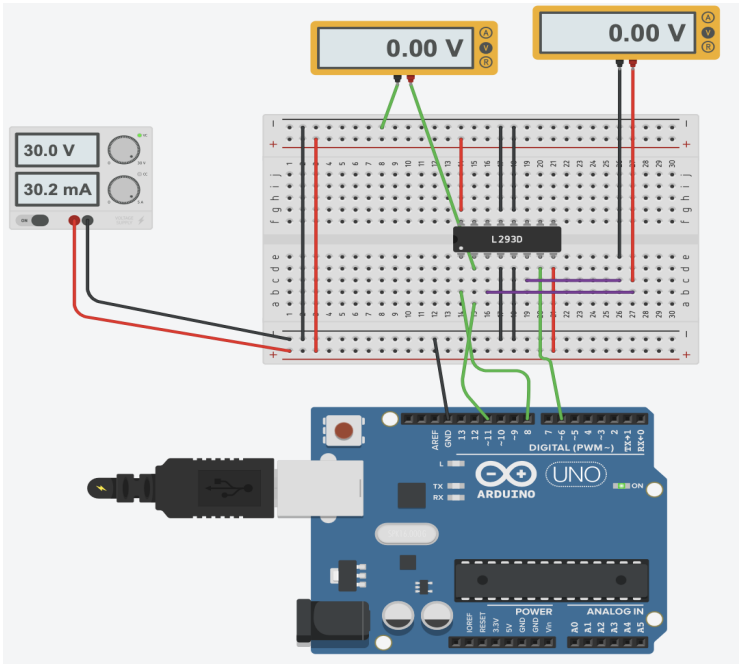

Figure 1.3: Schematic of the voltage-controller simulated in Tinkercad.

In the second design, the level in the liquid metal monopole was controlled by Arduino Uno and syringe pump. This setup is presented in Figure 1.4 and allow to control the monopole length in the tube. In the scheme, a basic three-volt pump is shown, and syringe will be connected later to provide directed liquid flow into the narrow cavity.

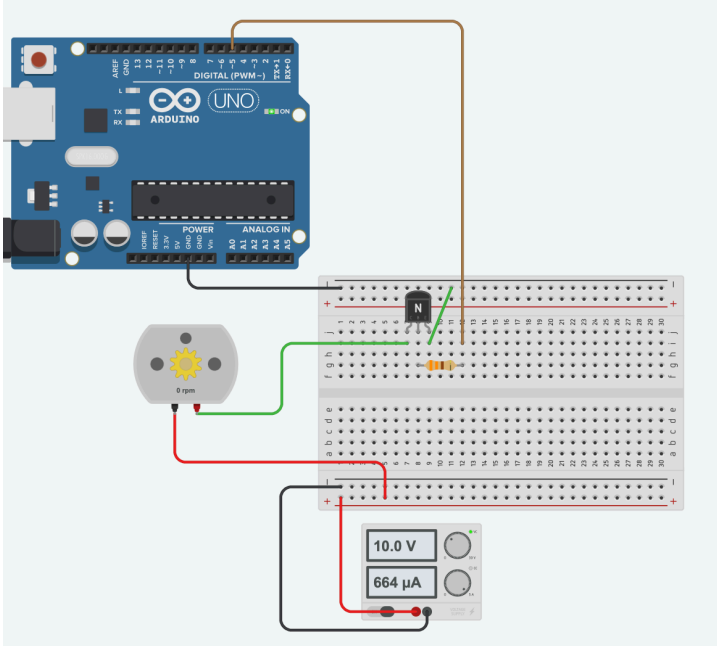

Figure 1.4: Schematic of the pump-controller in Tinkercad.

1.4.3 Fabrication process

The fabrication process of the antenna elements presented in Figure 1.5 and consists of material preparation, soldering and positioning stages.

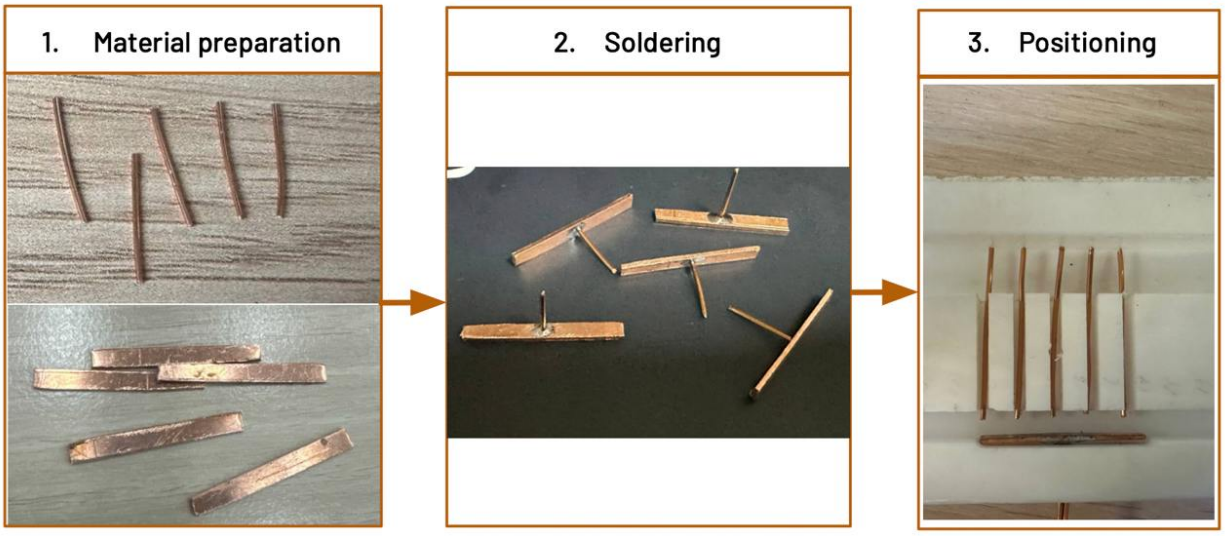

Figure 1.5 Three stages of the antenna elements fabrication process

In the material preparation, copper rods were cut from copper wire, copper plates were cut-out from copper sheet. All dimensions were observed according to the design parameters. Next,

electrical connection between copper rod and plate was created by using soldering. As the result, the busbars were obtained. In the positioning stage all copper elements were placed in Polytetrafluoroethylene (PTFE) mold.

After fabrication process, the Vector network analyzer (VNA) LiteVNA was connected to antenna. This device measure S_{11} - parameter and resonance frequency. The VNA were calibrated using industry-standard calibration kits to ensure measurement accuracy and repeatability.

Chapter 2 – Design of the FAS

A wide variety of structures, each suited to certain applications and performance standards, are included in the topic of antenna design. The number of antenna types is huge, ranging from the dipole antenna, which is known for its balanced radiation characteristics, to patch antennas, which are prized for their small size and integration capabilities [26]. Every design has different benefits and limitations with regard to size, radiation pattern, gain, and bandwidth. Among them, monopole antennas are known for their simplicity and ease of implementation.

Since the design and implementation of a fluid-antenna system is the main focus of this research, a monopole configuration of the antenna is the perfect suit this goal. Therefore, this literature review will specifically focus on the principles of monopole antenna design and optimization.

2.1 Design parameters

The monopole antenna is a vertical radiating element, typically a conductor, mounted over a ground plane. Its length is often a quarter-wavelength (λ/4) at the operating frequency. To calculate the wavelength (1) is used, where:

c - speed of the light, $3 \cdot 10^8$ m/s;

f - frequency, 2.4 GHz.

So, wavelength is $\lambda = 125$ mm, and length of the antenna is $\lambda/4 = 31.25$ mm.

$$\lambda = \frac{c}{f} \tag{1}$$

The quarter-wavelength monopole is a resonant antenna, so its input impedance of the antenna is about Z_i =36.5 Ω, which matches well with the 50 Ω standard transmission line.

2.2 Initial design: fluid-switchable monopole antenna array

The initial design approach focused on creating a fluid-switchable monopole antenna array operating at a target resonant frequency of 2.4 GHz. This design drew inspiration from the foundational work of Wong et al., which demonstrated the feasibility of using fluid metals for antenna reconfiguration. The core concept involved a linear array of copper monopole elements, each connected to a common feed point. To achieve port selection, a drop of Galinstan was employed as a fluid switch, selectively connecting the feed to monopole elements.

2.2.1 Antenna configuration

The antenna array consisted of five copper monopole elements, busbar and fluid metal drop. All five monopoles are with 1.5 mm diameter and 31.25 mm length, and arranged in a linear configuration. A busbar, with 31.25 mm length and 3 mm width, connects the monopoles to feed point though fluid drop. The ground plane was modeled as rectangular perfect electric conductor (PEC) with 100 mm × 100 mm dimensions. The ground plane provides a stable reference for the monopole elements. Figure 2.1 illustrates this design, showing the configuration of the copper monopole elements, the copper busbar, fluid metal drop and the ground plane.

To investigate the impact of element spacing on array performance, we systematically evaluated a range of spacings, varying from one wavelength down to 0.05 of a wavelength, and presented in the Table 2.

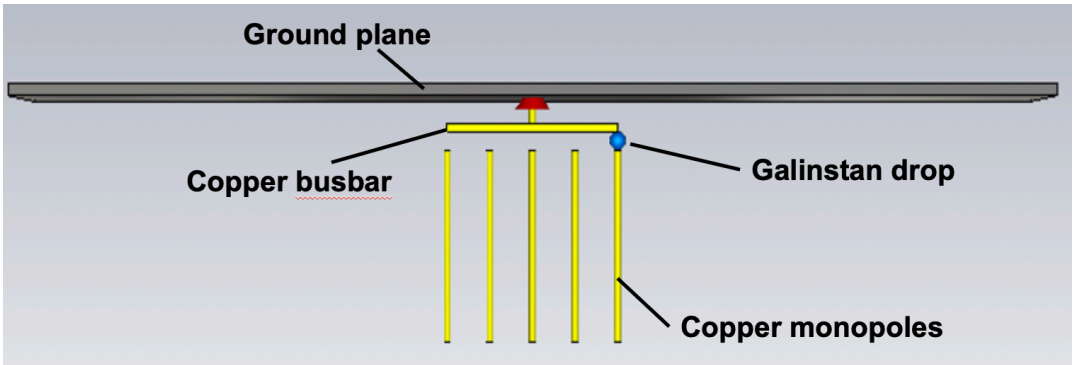

Figure 2.1: Design of the fluid-switchable monopole antenna array.

This comprehensive analysis allowed us to determine the optimal spacing for minimizing mutual coupling while maintaining a compact array size.

Figures 2.2, 2.3 and 2.4 depict the simulated S_{11}-parameter over the frequency across various element spacings for ports 1, 2, and 3, respectively. Ports 4 and 5 were discarded due to the same values between the first and fifth, second and fourth ports.

Table 2. Evaluation of Antenna Element Spacing

Equation	λ	0.5λ	0.25λ	0.1λ	0.05λ	0.01λ
Spacing, mm	125	62.5	31.25	12.5	6.25	1.25

Attention was paid to the results of the central monopole element (third port), as it was anticipated to exhibit the most accurate resonance frequency due to its symmetrical position within the array. First and second ports the same as fourth and fifth ports operate at the deviated frequency from the aiming. This deviation was attributed to the inherent electrical length of the antenna elements, which, due to their distance from the central element, resulted in a lower resonance frequency. Specifically, elements further from the center exhibited a longer electrical length, leading to a greater deviation from the desired 2.4 GHz.

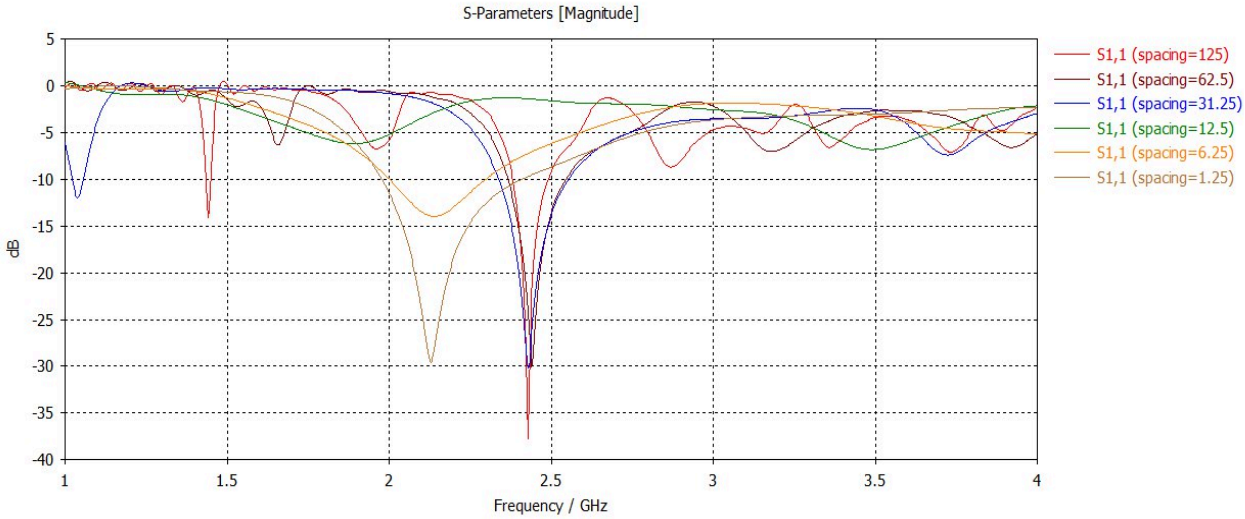

Figure 2.2: Graphical visualization of impact of different monopole spacing on S11-parameter for first port: 125 mm (red), 62.5 mm (brown), 31.25 mm (blue), 12.5 mm (green), 6.25 mm (yellow), 1.25 mm (ochre).

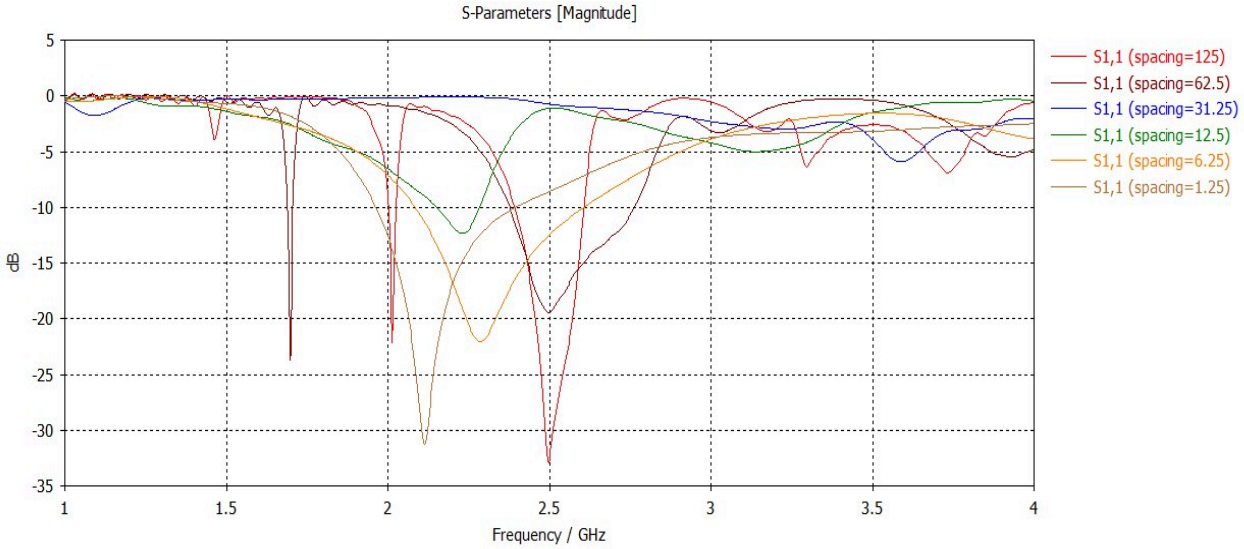

Figure 2.3: Graphical visualization of impact of different monopole spacing on S11-parameter for second port: 125 mm (red), 62.5 mm (brown), 31.25 mm (blue), 12.5 mm (green), 6.25 mm (yellow), 1.25 mm (ochre).

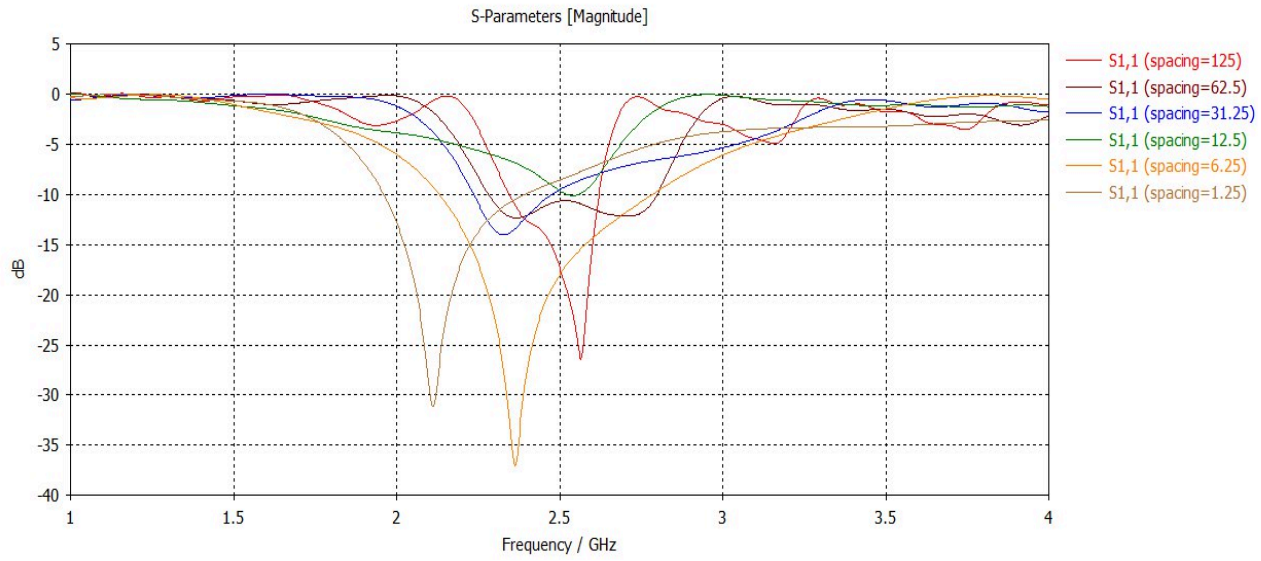

Figure 2.4: Graphical visualization of impact of different monopole spacing on S11-parameter for third port: 125 mm (red), 62.5 mm (brown), 31.25 mm (blue), 12.5 mm (green), 6.25 mm (yellow), 1.25 mm (ochre).

The results consistently demonstrate a significant impact of element spacing on the S_{11}-parameter. Notably, a spacing of 0.05λ emerged as the optimal choice, exhibiting the closest proximity to the desired resonance frequency of 2.4 GHz while maintaining excellent performance similarly for each port. For instance, while a spacing of 0.5λ yielded a resonance frequency close to 2.4 GHz at the third port, its corresponding S_{11}-parameter was only -12.22 dB, indicating suboptimal impedance matching and reduced efficiency. Moreover, at the second port it showed at least two resonance points at 1.7 GHz and 2.5 GHz. The same for spacing of 125 mm, that also showed resonance at the 2 GHz and 2.5 GHz frequency. Spacing of 0.25λ and 0.1λ showed low performance that was above -10 dB at some of the ports, which is unacceptable for stable antenna connection. In contrast, the 0.05λ spacing and 0.01λ achieved a significantly lower S_{11}-parameter, demonstrating superior performance and improved impedance matching. But spacing of 0.01λ shows no deviation in resonance frequency, which means that monopoles are too close to each other that due to mutual coupling they are forming one antenna operating at 2.11 GHz. The 0.05λ

spacing provide a balance between minimizing mutual coupling and maintaining a compact array size, resulting in optimal performance at the desired resonance frequency. Furthermore, the consistency of the results across all three ports (1, 2, and 3) confirms the reliability of this spacing. Therefore, a spacing of 0.05λ was selected for the fabrication of the fluid-switchable monopole antenna array.

After optimal linear spacing selection, the final configuration of the fluid-switchable monopole antenna array was simulated to verify its performance. Initial simulations revealed that the third port resonated at 2.366 GHz, slightly below the target frequency. The first and second ports resonated at 2.138 GHz and 2.287 GHz, respectively. To compensate for the deviations of ports further central and ensure all antenna elements operated at the same resonance frequency as the central element, a plan was devised to incorporate a phase-shifting block at the end of each antenna element in the prototype. This block would be designed to introduce a controlled phase shift, effectively reducing the difference in electrical length between the elements and aligning their resonance frequencies.

Still, the central monopole does not reach the target operating frequency. To address the initial 2.366 GHz resonance of the central element, the length of the monopole elements was adjusted. Through iterative simulations, it was determined that a final length of 30.84 mm resulted in a resonance frequency of 2.401 GHz, closely aligning with the target.

Figure 2.5 presents the simulated S_{11}-parameter for all ports at both the initial length (dashed curves) and the final adjusted length (solid curves). This figure demonstrates the shift in resonance frequency achieved through the length adjustment and highlights the improved performance of the antenna array at the target frequency of 2.4 GHz. After adding a phase-shifter at the end, other ports would be operating at the same parameters as central port.

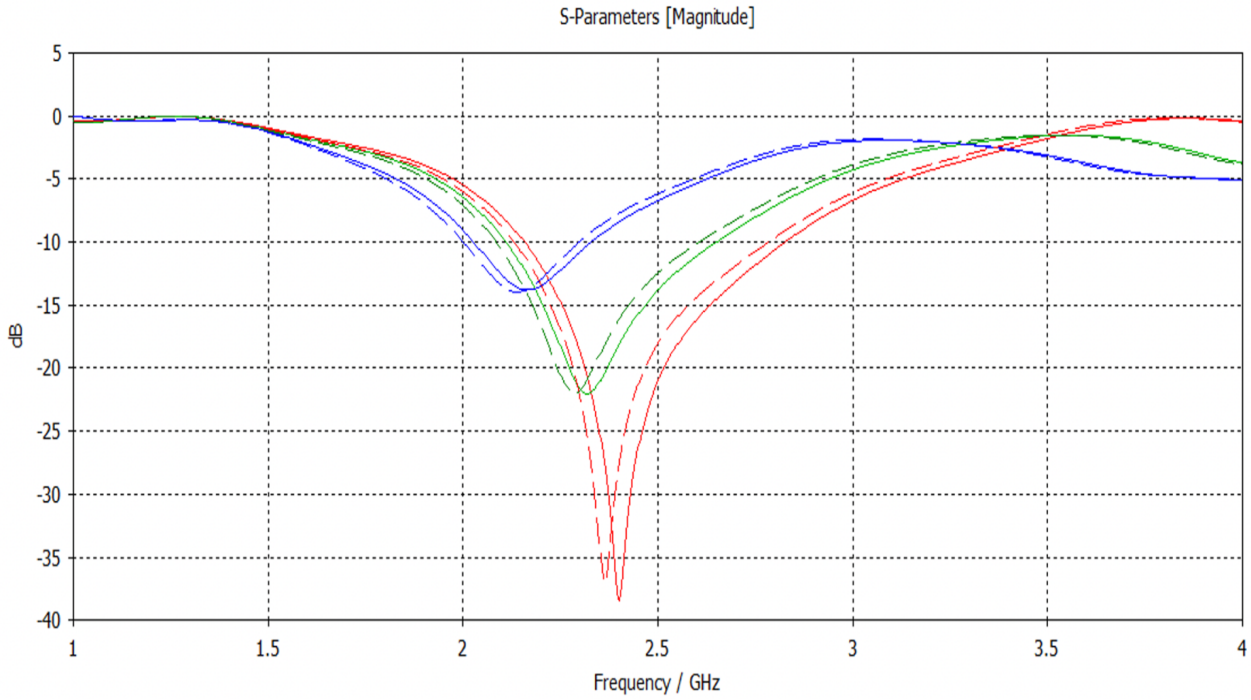

Figure 2.5: Simulation of S_{11}-parameter at initial length value (dushed curve) and final length value (solid curve) for each port (blue curves – first port, green curves – second port and red curves – third port).

2.2.2 Fluid-switch mechanism

Following the simulation and optimization of the antenna design's performance, the next crucial step was to evaluate the fluid-switching mechanism. It is crucial to create the effective mechanism to achieve dynamic port selection and beam steering within the fluid-switchable monopole antenna array. To this end, our initial investigation focused on the application of electrochemical capillary actuation as a means of controlling the Galinstan drop's movement. This system, presented in Figure 1.4, was built using L293 chip, Arduino Uno microcontroller and connecting wires.

The movement of the Galinstan drop was achieved through electrochemical capillary actuation. By applying a DC voltage across the Galinstan drop and the electrolyte, the surface tension of the liquid metal was manipulated. Specifically, the Galinstan drop exhibited motion

towards the positive bias, enabling selective connection to the desired monopole port. As the electrolyte Sodium Hydroxide (NaOH) is used. To facilitate control over the applied voltage and direction, an Arduino Uno microcontroller was employed. The Arduino Uno controlled an H-bridge circuit (L293D chip), which allowed for continuous adjustment of the voltage value and polarity.

2.3 Second design: reconfigurable liquid metal monopole array

Based on initial design, a second design approach was developed. This time, FAS is a fully reconfigurable liquid metal monopole array. In this design along with port selection, the frequency-reconfigurability is also achieved. The concept of the design is to create an array of liquid monopoles, where the length of each monopole could be dynamically controlled to adjust its resonant frequency.

2.3.1 Liquid Monopole

The design of the liquid monopole is presented in Figure 2.7. It consists of the cylindrical tube; liquid metal, injected into that tube; copper feed and copper ground plane. The polyvinylchloride (PVC) tube, with an 1 mm inner diameter and a 1 mm wall thickness, was filled with the Galinstan. Copper feed with 1 mm diameter, 10 mm length was placed at the bottom of the tube to connect with the rectangular PEC ground plane with dimensions of 100 mm x 100 mm. The discrete port of the antenna is installed between the ground plane and copper rod.

The length of the Galinstan monopole was varied from 18.75 mm to 75 mm, allowing for a wide range of frequency tuning. This length range was defined according to calculations using Eq. (1), which provides an operating frequency in the range from 1 GHz at 75 mm to 4 GHz at 18.75 mm length. The top of the tubes was open to allow for the injection of the Galinstan, and to allow for the adjustment of the Galinstan level.

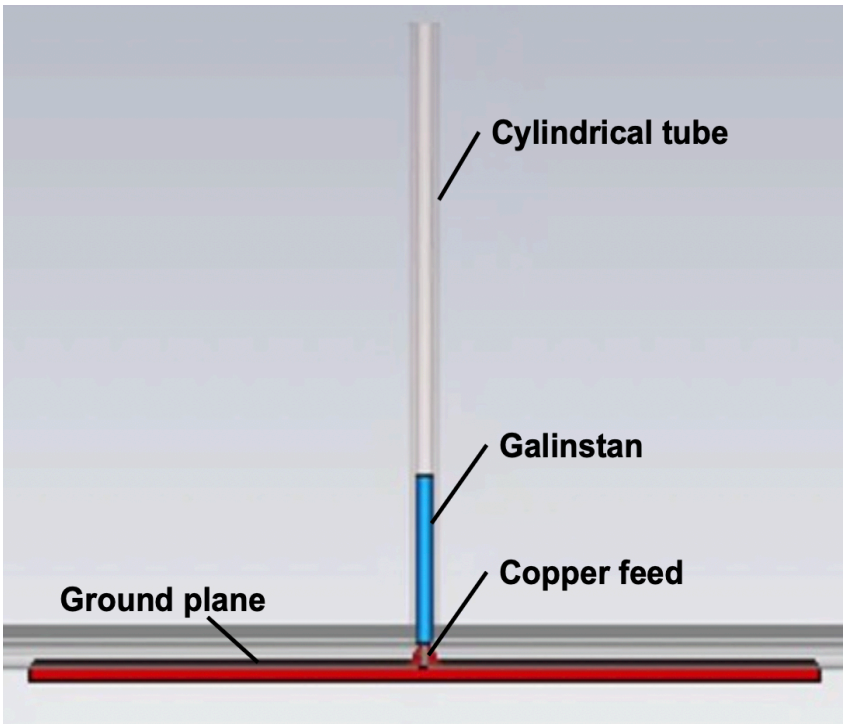

Figure 2.6: Design of the liquid monopole.

The simulations presented in Figure 2.8 demonstrated that a wide range of frequency tuning could be achieved by varying the Galinstan column length from 18.75 mm to 70.75 mm. Specifically, the resonant frequency was observed to decrease as the column length increased, indicating a lengthening of the effective electrical length. This tuning capability allowed for dynamic adaptation of the antenna array to different operating frequencies, making it suitable for applications requiring frequency agility. As it is shown, the range of 1- 3 GHz is obtained in a length range of 18.75 – 60.75 mm. When antenna length is 70.75 mm, its resonance at some point below 1 GHz and at 2.75 GHz, while according to Eq. (1) it should be 1.06 GHz and 2.12 GHz. Notably, with the length of 22.75 mm antenna has the better performance by almost 10 dBi.

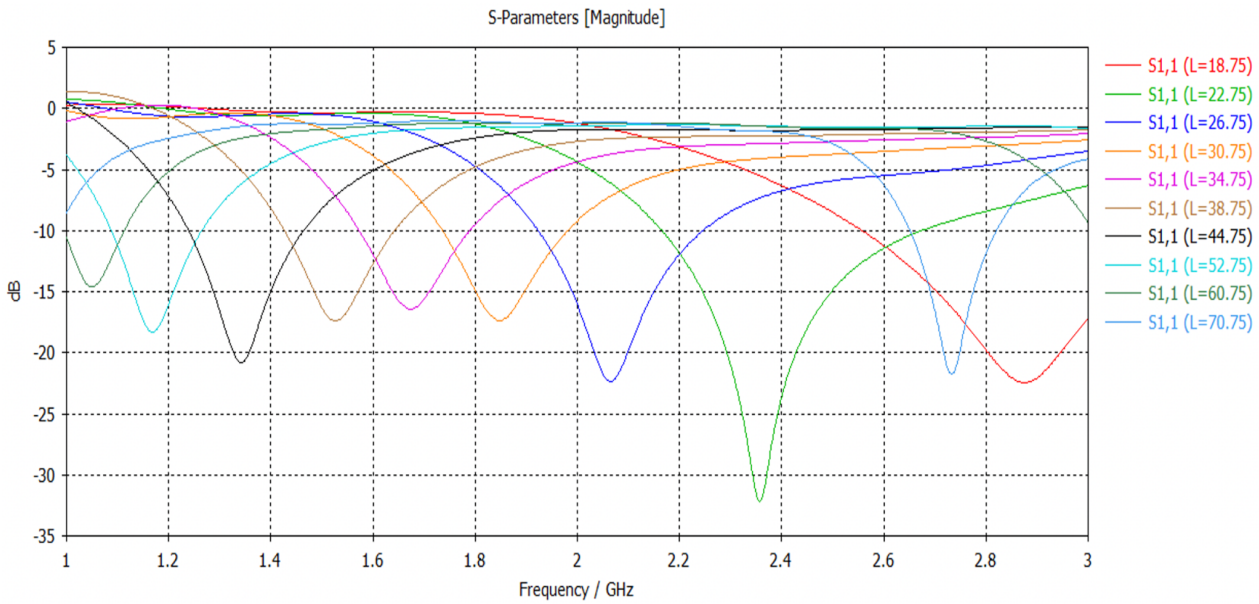

Figure 2.7: Simulation of S_{11}-parameter for adjusted length of the Galinstan.

2.3.2 Liquid Antenna Array Configuration

An array of one central liquid metal monopole (driven element) and four parasitic monopole elements was created, arranged in a linear configuration with a uniform spacing of 12.5 mm between their centers. All parasitic elements as well as liquid monopole utilizes a liquid metal, which length could be varied. The linear array configuration shown in Figure 2.9. The concept idea is to change the monopole performance that was designed in the previous section, by changing the level of the liquid metal in parasitic elements. These elements consist of the same tube with liquid Galinstan that is not connected to the feed point. Due to the mutual coupling, close location of the parasitic elements to the driven one it effects on the radiation of the antenna.

The array is capable to easily change the number of elements in the array from the one to five. In case its only one element – it is single-monopole mode, then parasitic element as reflector and/or director could be included or, otherwise, excluded. By changing the number of parasitics the adjustability in gain could be achieved. Also, it allows to achieve beam steering in X-axis.

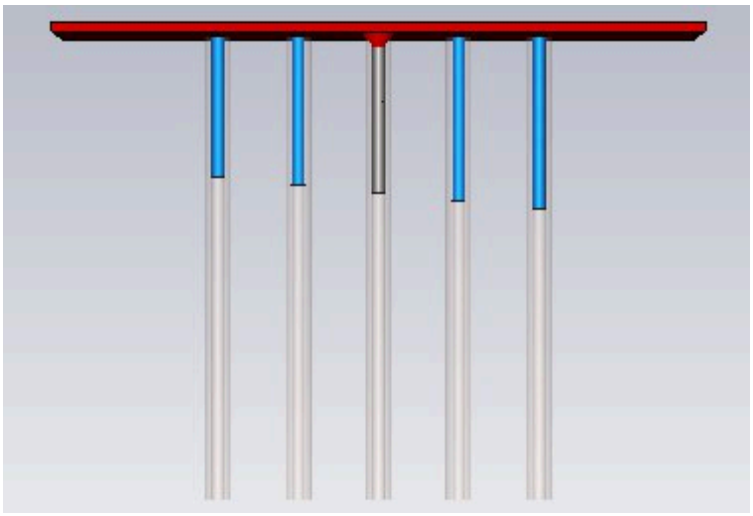

Figure 2.8: Design of the liquid monopole array antenna with five-monopole elements.

The adjustment of the Galinstan height is usually done with the implementing the pump system. The reconfigurability of the antenna array was further enhanced by the ability to independently control the Galinstan column length in each monopole element. This allowed for the creation of different radiation patterns across the array, by easily switching every element's mode to reflector, director or just empty it.

While simulations, the length of the driven monopole that operate at 2.4 GHz was obtained. As a result, length of the driven element is 24.25 mm, length of the reflector is bigger for 5% and length of the director 5% shorter.

As we see from the Table 3. the gain of the antenna is varying from 3.309 to 5.060 dBi, giving the maximum increase in gain of 1.751 dBi. The number of both director and reflector affects on increasing or decreasing the gain. If increasing the director number gives gain increase of 0.524 dBi, the increase in reflector number gives increase of 0.376 dBi. However, adding reflectors give overall increase in gain higher than adding directors: 1.190 dBi for directors versus 1.751 dBi for reflectors. The results in the table presented only for $\varphi = 90°$, but for $\varphi = -90°$ the obtained results are the symmetrically same.

Table 3. The simulation results of liquid-monopole array with different linear configurations.

L_1, mm	L_2, mm	L_3, mm	L_4, mm	L_5, mm	S_{11}, dB	Gain
-	-	24,25	-	-	-27,75	3,309
-	23,04	24,25	-	-	-23,11	3,850
21,89	-	24,25	-	-	-23,30	3,975
21,89	23,04	24,25	-	-	-14,90	4,499
25,46	-	24,25	-	-	-18,35	4,520
26,74	-	24,25	-	-	-17,35	4,684
26,74	25,46	24,25	-	-	-11,47	5,060
26,74	25,46	24,25	23,04	21,89	-8,78	4,082

Chapter 3 – Prototyping and Experimental Evaluation

To verify the proposed designs, hardware prototypes of the both antennas were fabricated and measured. A vector network analyzer was used for the measurement.

The fabrication of the fluid-switchable monopole antenna array involved several key steps, focusing on the precise construction of the copper elements, the integration of the fluid-switch mechanism, and the assembly of the ground plane.

3.1 Monopole array prototype

For the hardware prototype of the monopole array antenna was fabricated all copper elements according to Figure 1.3 and created a special mold from PTFE. This mold has a cut-out place for installation of busbar, copper monopoles and channel for liquid between them. This will help to make the construction of the antenna more stable and rigid. Because, without it the monopoles are bend too easily while construction, due to soft property of copper.

The monopole elements were fabricated from 1.5 mm diameter copper wire, carefully cut to a precise length of 30.84 mm. Each rod was carefully polished to minimize surface roughness and ensure a consistent electrical contact.

A custom-designed copper busbar was machined to provide a uniform distribution of current to all monopole elements. The plate part of the busbar was cut-out from copper sheet with 1 mm thickness with the length of 30.84 mm and width of 3 mm. Then, a copper rod with diameter 1.5 mm and length of 4 mm was soldered to the center of the copper plate. As a result, a busbar that could be connected to the ground plane and SubMiniature version A-connector (SMA-connector) was obtained. All received copper elements were carefully installed in their niches in the mold and fluid drop was added in the cavity as shown in the Figure 3.1.

Figure 3.1: Copper elements and fluid drop of the Galinstan installed in the mold.

After fabrication process, the prototype was connected to the LiteVNA device to measure the S_{11}-parameter over frequency to obtain the performing parameter of the antenna and port selection ability. The Table 4 presents a experimental evaluation of the performance characteristics of a prototype and a simulated antenna with different ports connected through fluid-drop.

Table 4. Performance characteristics (S_{11} and resonance frequency) of prototype and simulated liquid antenna at different ports

#	Number of the port	Resonant frequency f_{res}, GHz	Simulated resonant frequency f'_{res}, GHz	S_{11}-parameter, dB	Simulated S'_{11}-parameter, dB
1	1	0,922	2,4	-24,70	-37,25
2	2	0,922	2,836	-21,14	-22,02
3	3	0,922	1,747	-20,35	-15,96
4	4	0,922	1,591	-19,11	-15,60
5	5	0,952	1,459	-22,12	-16,84

As it shown in Table 4, the fabricated prototype shows significant deviations in operating frequency from the simulated antenna performance. Notably, the measured resonance frequency

is lower than the target, approximately 1 GHz over 2.4 GHz. Moreover, the resonance frequency remains consistent regardless of the port selected, suggesting that the measurement is likely dominated by the busbar's operating frequency, rather than the intended monopole activation. This implies that the fluid-drop, despite its application, is not successfully establishing an electrical connection to either of the monopoles. Adding to these challenges, the fluid-drop demonstrates a strong tendency to adhere to the busbar surface, even after NaOH-treatment aimed at promoting droplet mobility. This persistent adhesion further hinders the practical implementation of the intended switching mechanism.

3.2 Actuator prototype

To move the Galinstan drop along the channel, we used an Arduino Uno and a special circuit called an H-bridge. This setup let us change the voltage and direction of the electricity, which controlled the Galinstan drop. The Arduino Uno was programmed to adjust the voltage as needed to keep it moving correctly. The assembled circuit is shown in Figure 3.1 and fully reflects its simulation, and enabled fine-tuned manipulation of the Galinstan drop's position, ensuring reliable and repeatable switching between the monopole ports. Before connecting the actuator setup with the antenna, we experimentally evaluated the necessary voltage parameters and liquid properties in the controlling environment without adding any antenna details. For this, the following experiment was conducted: we actuated just a fluid drop and looked for the dependence of its movement on such parameters as the concentration of the solution, the mass of the drop, and the voltage value.

Experiment was conducted in a PTFE mold. At both ends of the stroke, copper contacts were placed and connected with a voltage-controller unit. The controller itself was connected to the power supply, that is then was adjusted by the L293 chip and transmitted to the copper contacts

in the mold. Into the channel, the NaOH solution was poured. Subsequently, the liquid metal droplet of Galinstan was added into the channel. The length of the droplet stroke was 15 cm. The setup is shown in Figure 3.2.

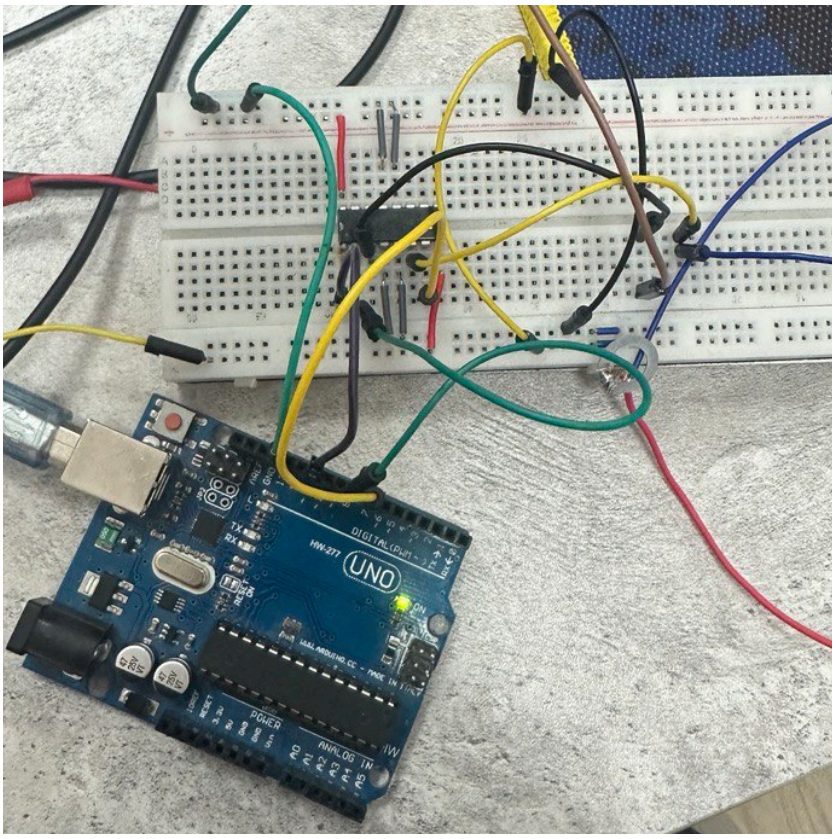

Figure 3.2: Developed setup for the voltage-controlled actuator.

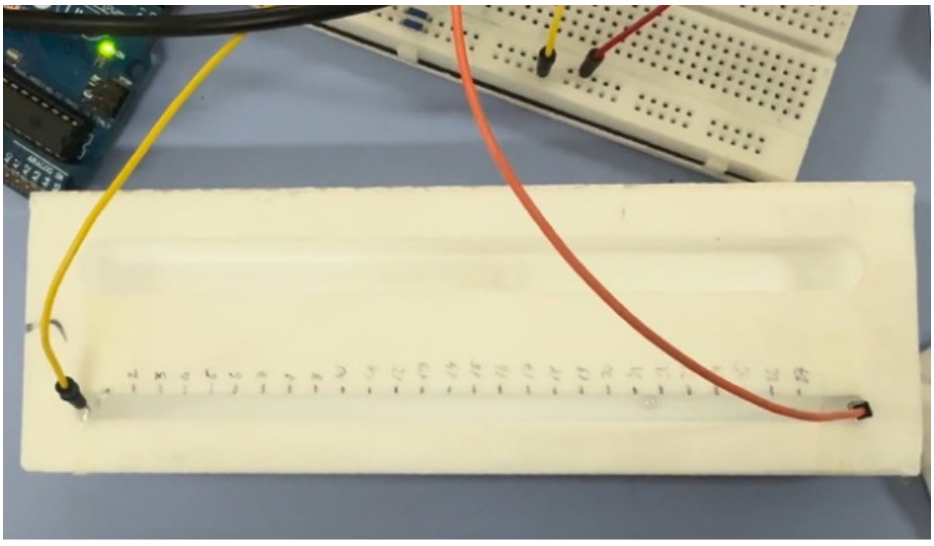

Figure 3.3: Experimental setup for the ECA.

The droplet mass was measured at each iteration of the experiment, to ensure equal conditions, in which it was 6 g. Then the velocity of this droplet was calculated at each voltage value. After analyzing these data, we obtain a table showing the dependence of the droplet speed on the voltage.

As shown in Figure 3.4, the dependence of speed on voltage is mainly direct. This trend was clearly visible at high voltage values, where the dependence increases proportionally (Figure 3.3, 1). At small values (up to 10 V), the speed increased insignificantly (Figure 3.3, 3). It was also noted that the longer the experiment was conducted, the more stable was the droplet speed (Figure 3.3, 2). This result was attributed to the fact that the longer we applied the voltage to the NaOH solution, the more the concentration of ions changed, affecting the movement of the droplets. Concentration change happens, because hydrogen and oxygen gasses are produced at the cathode and anode, respectively, and bubble out of the solution. Also, it was observed that the color of the electrolyte solution changed from transparent to the yellow color after the experiment.

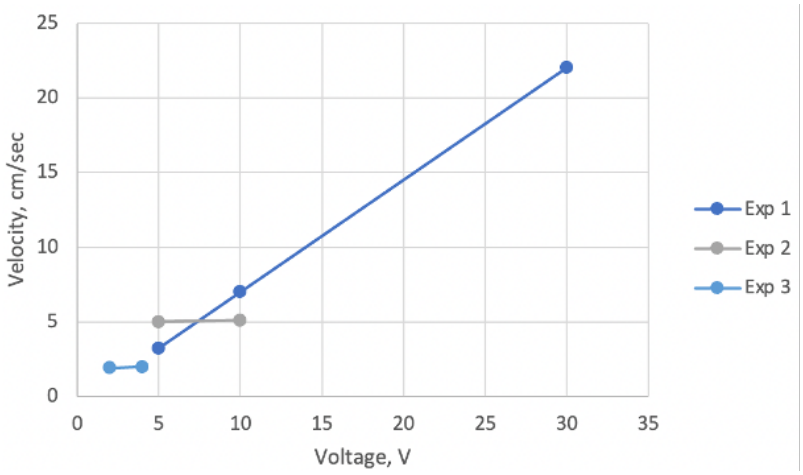

Figure 3.4: Dependence of the drop velocity on voltage, where: 1) experiment conducted at high voltages; 2) experiment lasted for 5 minutes; 3) experiment conducted at low voltages.

That is why, it was decided to apply another method of actuating the liquid metal drop. To maintain this aim the automatic actuation of liquid metal using a Arduino-based controllable air

pump has been fabricated. This pump can change the position of the fluid drop, allowing it to quickly find the best port. Such systems can be more practical and compact if a micropump is used in their place.

3.3 Prototype of the reconfigurable liquid metal monopole array

A hardware fluid-monopole antenna was developed as it is presented in Figure 3.5. It was constructed using polyvinyl chloride (PVC) tubes with a Galinstan liquid metal inner core as a prototype. At the bottom of the tube was placed a copper feed with 10 mm length and then connected to an SMA-connector. The ground plane from 100 mm x 100 mm copper sheet with 1 mm thickness was used. To connect antenna with ground plane, the hole with 7 mm diameter o in the center of the ground plane and the SMA-connector was soldered in it.

Transparent flexible tube made of medical grade PVC was used to create a cylindrical device with an inner diameter of 2 mm and length 73.75 mm. Then the Galinstan was injected slowly via a long 23-gauge stainless steel needle tip with 0.33 mm inner and 0.65 mm outer diameter into the 2.8 mm cavity until it was filled.

Initially, an attempt was made to inject liquid metal through a syringe into an open PVC tube. However, the antenna failed to achieve the desired uniformity. The reason for that is the Galinstan's high surface tension. That is why, to avoid the uneven coating of the metal and its sticking to tube surface, the Galinstan was pre-treated with sodium hydroxide (NaOH) solution. NaoH acts as a buffer and prevent the direct contact between Galinstan and PVC tube’s inner surface. This provide more controlled and uniform filling process.

After fabrication process, the prototype was connected to the LiteVNA device to measure the S_{11}-parameter over frequency to obtain the performing parameter of the antenna and frequency-

tuning ability. The Table 5 presents a comparison of the performance characteristics of a prototype and a simulated liquid antenna at different lengths of the liquid monopole.

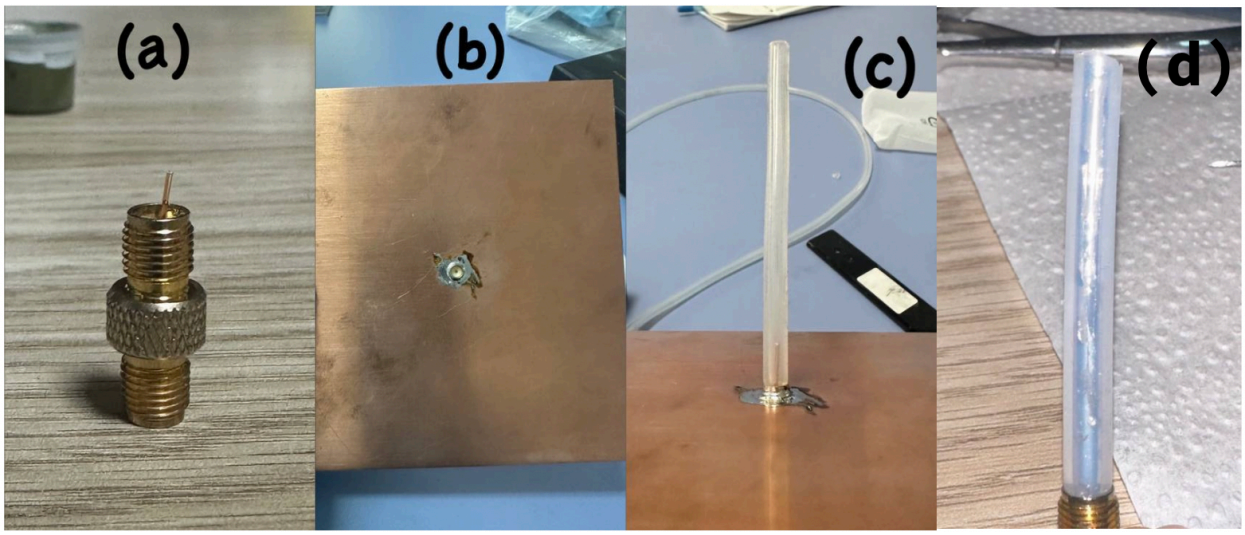

Figure 3.5: The fabricated step of frequency-tunable monopole: a) connecting copper wire with SMA-connector; b) soldering the SMA-connector to the center of ground plane; c) connecting PVC tube to the feed and SMA-port; d)filling tube with the Galinstan.

Generally, as the length of the liquid monopole (L) increases, the resonant frequency (both measured and simulated) decreases. Notably, the S_{11} values of the prototype is lower than simulated ones, which indicates better impedance matching at the resonant frequency, meaning more power is being radiated and less is reflected back. However, the simulated resonant frequency shows a significant deviation from the measured value, although the deviation has decreased with increasing length.

This suggests that the simulation model may not fully reflect all the physical characteristics of the fabricated prototype. Several factors may contribute to these deviations. One of the issues in the prototype may be the effect of the NaOH solution that was used to facilitate the controlled movement of the Galinstan. NaOH itself and its interaction with the Galinstan inside the PVC tube of the monopole may have altered the effective electrical properties of the liquid metal or dielectric

medium. This may have resulted in shifts in the resonant frequency compared to the simulation assuming pure Galinstan inside the PVC.

Table 5. Performance characteristics (S_{11} and resonance frequency) of prototype and simulated liquid antenna at different lengths

#	Length of the liquid monopole L, mm	Resonant frequency f_{res}, GHz	Simulated resonant frequency f'_{res}, GHz	S_{11}-parameter, dB	Simulated S'_{11}-parameter, dB
1	18,5	2,491	3,18	-36,74	-29,49
2	21,0	2,387	2,836	-33,56	-22,02
3	35,0	1,504	1,747	-30,51	-15,96
4	39,0	1,520	1,591	-21,85	-15,60
5	43,0	1,370	1,459	-27,40	-16,84
6	50,0	1,131	1,264	-12,67	-19,96

Another potential issue may be non-uniform coating or distribution of the Galinstan inside the PVC tube, especially over longer lengths. Although efforts were made to ensure uniform filling, variations in the inner surface of the tube or the injection process may have resulted in non-ideal geometry. Such irregularities may affect the current distribution along the monopole and therefore alter its resonant frequency and impedance matching characteristics.

References

[1] X. Lin, H. Yang, Y. Zhao, J. Hu and K. -K. Wong, "Performance Analysis of Integrated Data and Energy Transfer Assisted by Fluid Antenna Systems," *ICC 2024 - IEEE International Conference on Communications*, Denver, CO, USA, 2024, pp. 2761-2766, doi: 10.1109/ICC51166.2024.10622204.

[2] W. K. New, K. K. Wong, H. Xu, K. F. Tong and C. B. Chae, "Fluid Antenna System: New Insights on Outage Probability and Diversity Gain," in IEEE Transactions on Wireless Communications, vol. 23, no. 1, pp. 128-140, Jan. 2024, doi: 10.1109/TWC.2023.3276245.10130117

[3] Dong, Yuandan and Tatsuo Itoh. "Metamaterial-Based Antennas." *Proceedings of the IEEE* 100 (2012): 2271-2285.

[4] H. Xu, K. -K. Wong, W. K. New and K. -F. Tong, "On Outage Probability for Two-User Fluid Antenna Multiple Access," *ICC 2023 - IEEE International Conference on Communications*, Rome, Italy, 2023, pp. 2246-2251, doi: 10.1109/ICC45041.2023.10279640.

[5] K.K. Wong, A.Shojaeifard, K.F. Tong and Y.Zhang, "Performance Limits of Fluid Antenna Systems." in *IEEE Communications Letters* 24, 2020: 2469-2472.

[6] F. Tariq, M. R. A. Khandaker, K. -K. Wong, M. A. Imran, M. Bennis and M. Debbah, "A Speculative Study on 6G," in *IEEE Wireless Communications*, vol. 27, no. 4, pp. 118-125, August 2020, doi: 10.1109/MWC.001.1900488.

[7] K. -K. Wong, A. Shojaeifard, K. -F. Tong and Y. Zhang, "Fluid Antenna Systems," in *IEEE Transactions on Wireless Communications*, vol. 20, no. 3, pp. 1950-1962, March 2021, doi: 10.1109/TWC.2020.3037595.

[8] K. -K. Wong and K. -F. Tong, "Fluid Antenna Multiple Access," in *IEEE Transactions on Wireless Communications*, vol. 21, no. 7, pp. 4801-4815, July 2022, doi: 10.1109/TWC.2021.3133410.

[9] Y. Huang, L. Xing, C. Song, S. Wang and F. Elhouni, "Liquid Antennas: Past, Present and Future," in *IEEE Open Journal of Antennas and Propagation*, vol. 2, pp. 473-487, 2021, doi: 10.1109/OJAP.2021.3069325.

[10] G. J. Hayes, J. -H. So, A. Qusba, M. D. Dickey and G. Lazzi, "Flexible Liquid Metal Alloy (EGaIn) Microstrip Patch Antenna," in *IEEE Transactions on Antennas and Propagation*, vol. 60, no. 5, pp. 2151-2156, May 2012, doi: 10.1109/TAP.2012.2189698.

[11] C. Psomas, P. J. Smith, H. A. Suraweera and I. Krikidis, "Continuous Fluid Antenna Systems: Modeling and Analysis," in *IEEE Communications Letters*, vol. 27, no. 12, pp. 3370-3374, Dec. 2023, doi: 10.1109/LCOMM.2023.3330157.

[12] L. Song and Y. Rahmat-Samii, "Reconfigurable Patch Antenna with Liquid Metal Tuning Slots and 3D Printed Microfiuidics," *2018 IEEE International Symposium on Antennas and Propagation & USNC/URSI National Radio Science Meeting*, Boston, MA, USA, 2018, pp. 289-290, doi: 10.1109/APUSNCURSINRSM.2018.8608719.

[13] J. O. Martínez, J. R. Rodríguez, Y. Shen, K. -F. Tong, K. -K. Wong and A. G. Armada, "Toward Liquid Reconfigurable Antenna Arrays for Wireless Communications," in *IEEE Communications Magazine*, vol. 60, no. 12, pp. 145-151, December 2022, doi: 10.1109/MCOM.001.2200392.

[14] S. Dash, C. Psomas, I. Krikidis, "Selection of metallic liquid in sub-6 GHz antenna design for 6G networks," *Sci Rep* **13**, 20551 (2023). https://doi.org/10.1038/s41598-023-47870-7

[15] K. N. Paracha, A. D. Butt, A. S. Alghamdi, S. A. Babale, P. J. Soh, "Liquid Metal Antennas: Materials, Fabrication and Applications," *Sensors*, *20*(1), 177, 2020, https://doi.org/10.3390/s20010177

[16] H. Abu Bakar, R. Abd Rahim, P. J. Soh, P. Akkaraekthalin, "Liquid-Based Reconfigurable Antenna Technology: Recent Developments, Challenges and Future," *Sensors*, *21*(3), 827, 2021, https://doi.org/10.3390/s21030827

[17] V. Bharambe, D. P. Parekh, C. Ladd, K. Moussa, M. D. Dickey and J. J. Adams, "Liquid-Metal-Filled 3-D Antenna Array Structure With an Integrated Feeding Network," in *IEEE Antennas and Wireless Propagation Letters*, vol. 17, no. 5, pp. 739-742, May 2018, doi: 10.1109/LAWP.2018.2813309.

[18] Y. W. Wu, S. Alkaraki, S. Y. Tang, Y. Wang, J. R. Kelly, "Circuits and antennas incorporating gallium-based liquid metal," *Proceedings of the IEEE*, *111*(8), 955-977, 2023

[19] M. R. K. M. D. D. M.Wang, C. Trlica, M. R. Khan, M. D. Dickey, J. J. Adams, "A reconfigurable liquid metal antenna driven by electrochemically controlled capillarity," *Journal of Applied Physics*, *117*(19), 2015

[20] Y. Shen, K. F. Tong, K. K. Wong, "Reconfigurable surface wave fluid antenna for spatial MIMO applications," 2021 IEEE-APS Topical Conference on Antennas and Propagation in Wireless Communications (APWC). – IEEE, 2021. – C. 150-152.

[21] N. S. Jeong, A. Koh, "Liquid Metal Broadband Monopole for Stretchable Electronics," *2019 IEEE International Symposium on Antennas and Propagation and USNC-URSI Radio Science Meeting*, Atlanta, GA, USA, 2019, pp. 763-764, doi: 10.1109/APUSNCURSINRSM.2019.8888557.

[22] A. Dey, R. Guldiken and G. Mumcu, "Microfluidically Reconfigured Wideband Frequency-Tunable Liquid-Metal Monopole Antenna," in *IEEE Transactions on Antennas and Propagation*, vol. 64, no. 6, pp. 2572-2576, June 2016, doi: 10.1109/TAP.2016.2551358.

[23] N. Jackson, J. Buckley, C. Clarke, "Manufacturing methods of stretchable liquid metal-based antenna," *Microsyst Technol* **25**, 3175–3184 (2019). https://doi.org/10.1007/s00542-018-4234-2

[24] D. Kim, R. G. Pierce, R. Henderson, S. J. Doo, K. Yoo, J. B. Lee, "Liquid metal actuation-based reversible frequency tunable monopole antenna," *Applied Physics Letters*, *105*(23), 2014

[25] Y. Zhang, S. Lin, B. Li, Q. Ding, Z. Fan and X. Zhang, "Simulation Design of Pattern Reconfigurable Antenna Based On Liquid Metal Switch," *2022 IEEE International Symposium on Antennas and Propagation and USNC-URSI Radio Science Meeting (AP-S/URSI)*, Denver, CO, USA, 2022, pp. 1200-1201, doi: 10.1109/AP-S/USNC-URSI47032.2022.9886113.

[26] W. K. New, K. K. Wong, H. Xu, C. Wang, F. R. Ghadi, J. Zhang, K. F. Tong, "A tutorial on fluid antenna system for 6G networks: Encompassing communication theory, optimization methods and hardware designs," *IEEE Communications Surveys & Tutorials, 2024*